Article:

Rehman, A.U., Worden, K. orcid.org/0000-0002-1035-238X and Rongong, J.A. orcid.org/0000-0002-6252-6230 (2016) On Crack Detection in Tuned and Mistuned Repeating Structures Using the Modal Assurance Criterion. Strain, 52 (3). pp. 175-185. ISSN 0039-2103

https://doi.org/10.1111/str.12177

Crack Detection in Tuned and Mistuned Repeating Structures using the Modal Assurance Criterion

Anees U Rehman[1], Keith Worden[2], Jem A Rongong[2]

[1] Department of Mechanical Engineering, University of Engineering and Technology, Lahore, Pakistan.

[2] Dynamics Research Group, Department of Mechanical Engineering, University of Sheffield, Sheffield S1 3JD, UK.

Corresponding Author

Anees U Rehman

Department of Mechanical Engineering, University of Engineering and Technology, Lahore, Pakistan.

a.u.rehman@uet.edu.pk

Tel: +92 321 4974215

Abstract

Repeating structures in the form of multiple-bladed rotors are used widely in turbomachinery. Mistuning in turbomachinery is caused by small differences in individual blade properties due to inevitable material and manufacturing variations, resulting in the splitting of vibration modes of the tuned system. Modal characteristics of the blades are quite sensitive to the level of mistuning present inside the structure. In addition, the existence of damage also results in changed dynamics of the complete system. This paper introduces a Modal Assurance Criterion (MAC)-based approach for the investigation of small defects such as cracks in a repeating structure. In order to understand the key issues involved, initial work involved a numerical study of a simple comb-like repeating structure, followed by a detailed numerical and experimental investigation of a tuned and mistuned bladed disc. Changes to the system modeshapes and mode order arising from damage are related to the location and severity of damage. Damage, in the form of small, open cracks, is modelled using different techniques such as: material removal, monotonic reduction in the modulus of elasticity of selected elements at the required location, and mass modification. Damage indices based on differences in the MAC that give a measure of the change in the modeshapes are introduced. MAC matrices are obtained using a reduced number of data points. The damage index is obtained from the Frobenius norm of the MAC matrix subtracted from the AutoMAC of a reference tuned model without crack. A clear correlation between the damage indices and crack depth / location is shown. Application of this approach to the limited data obtainable from developing techniques such as blade tip-timing is also explained.

Keywords

Damage detection, Modal Assurance Criterion (MAC), natural frequency, mode shapes, mistuning.

1 Introduction

Mechanical vibrations are a significant source of possible failure in rotating machines such as gas turbines operating in both the power generation and aerospace industries. Gas turbines blades have always been vulnerable to the severe dynamic loads experienced during operation which can include engine order excitation along with nominally random vibrations. The dynamic response can increase considerably if some abnormality is developed within the operating system, such as the initiation of a crack in a blade, leading to increased risk of fatigue failure. Also, if a crack is allowed to grow in one of the blades of a rotor system, catastrophic failure could occur due to the high value of the rotation-induced stresses. For safe operation therefore, cracks should be detected during crack initiation or in the early propagation stage, well before ultimate failure occurs.

Because of its importance, many researchers have studied crack detection in structures. Different non-destructive testing techniques have been used for detecting cracks in turbomachine blades, including: dye penetrant, eddy current inspection, radiography, ultrasonic methods, shearography and thermography [1]. While these methods are highly reliable, they are not always convenient to use on assembled turbomachinery, particularly if it is in operation. An alternative approach is to infer damage from changes in the vibration characteristics of the system [2,3]. Important issues affecting success of such a strategy include the type and location of the crack, the vibration mode shapes considered and the presence of other system-changing factors.

Cracks reduce the stiffness of a structure locally which in turn leads to reduced natural frequencies and altered mode shapes. Changes in the modal characteristics may not be the same for each mode as they depend on the size and location of the crack [4]. For example, a crack will create a larger drop in frequency if it is located in a zone of high modal curvature such as the clamped end of a cantilever [5]. Selection of the best suited vibration modes for damage detection has been a conflicted issue in the past. While many researchers [4, 6] have considered the use of lower vibration modes as they are most easily identified, others [4, 7] have argued in favour of selecting higher vibration modes as they are more sensitive to low levels of damage. Another approach is to select modes of interest based on the expected sensitivity obtained by calculating the modal masses and participation factors of a given range of modes [8]. However, detecting damage on frequency change alone is challenging because the natural frequency is proportional to the square root of stiffness and therefore relatively large stiffness change is required before significant frequency change can be detected.

The condition of the crack also influences the dynamic response. If the crack remains open (i.e. the faces do not come in contact) the entire time, it acts as a simple stiffness reduction. However, if during operation opening and closing occurs (faces come into contact), significant nonlinearity in stiffness and damping can arise. Due to the presence of nonlinear effects in the output response, nonlinear output frequency response functions have been shown to be a sensitive indicator of the presence of a crack as compared to frequency response functions [9].

The role of environment-induced effects, such as changes in stiffness and dimensions due to temperature, in complicating vibration-based damage identification procedures is well known. For structures with many, nominally identical elements, the phenomenon of mistuning affects the dynamic response. Mistuning arises from minute differences in the geometric and/or material properties of each individual element and is inevitable due to manufacturing tolerances. Structural mistuning results in significantly changed mode shapes and widening of the resonance frequency range in forced response. Different mistuning patterns have different effects on the mechanical behaviour of the system. It has been shown that alternate mistuning can improve the flutter stability of the blades as compared to random mistuning. In the presence of random mistuning, stabilisation of the system is again highly dependent on the particular random mistuning pattern [10]. The relationship between tuned free vibration characteristics and operating conditions on one hand, and mistuning sensitivity on the other hand can be derived by utilising an eigenfrequency verses number of nodal diameters plot [11]. A significant limiting factor in the analysis of mistuned repeating structures is the computational effort required as each unit is slightly different. Model reduction techniques such Component-Mode-based methods and System-Mode-based methods [12] are often used to alleviate this problem when carrying out numerical forced response analyses.

In this paper, a method of detecting open cracks in repeating structures is studied in tuned and mistuned environments. Two representative multi-bladed structures are considered: a straight comb-type structure and an idealised bladed disc. The comb structure is first used to develop a suitable modelling approach and to investigate the effectiveness of a damage index based on the Modal Assurance Critereon (MAC) that highlights changes in mode shape and mode order. The bladed disc is slightly more complicated in that it displays cyclic symmetry which requires the development of an additional procedure to allow mode correlation. Using this model, the variation of the damage index is investigated for tuned and mistuned conditions as the crack depth and location are changed. Comparisons with experimental results on a physical bladed disc are used to justify the modelling approach and the levels of mistuning considered.

2 Development of the MAC-based damage detection approach

A bladed rotor or stator set in a turbine engine is a cyclically symmetric structure which is complex in geometry and vibration behaviour. To retain generality and minimise computational cost this work studied the behaviour of considerably simplified models that retain the key features: a number of nearly-identical flexible blades connected together by a stiff base. The damage detection approach was first developed using a numerical model of a two-dimensional comb-like structure comprising eight evenly spaced, identical blades mounted on a thick base. A sketch is presented in Figure 1.

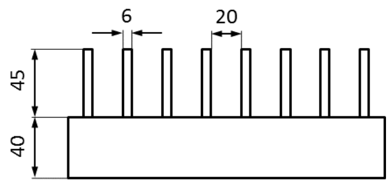

Figure 1: Geometry of comb structure

2.1 Finite element model

Finite element (FE) models were constructed and meshed using two-dimensional, plane stress quadrilateral elements with eight nodes. In each case, material properties assigned to the FE models approximated the behaviour of medium carbon steel with Young's modulus E = 200 GPa, Poisson's ratio $\upsilon = 0.3$ and density $\rho = 8000$ kg/m^3. Pinned boundary conditions were applied to single nodes half-way up each side of the base. Neither material nor geometric nonlinearities were defined as modal analysis ignores any such nonlinearity. For the same reason, no slippage was allowed at the interface between the base and the blades. Eigenvalue analyses were run with a range of different mesh densities and the final mesh selected was the coarsest one that predicted natural frequencies of the first ten modes to within 0.5% of the asymptotic value.

The first ten natural frequencies and modes shapes of the comb structure are presented in Figure 2. It can be seen that Modes 1 and 10 are bending modes of the base. Modes 2 to 9 are a family of modes in which the base has negligible motion while the deflected shape of each blade resembles the first flexure mode of a cantilever beam. Note that there are as many modes in this family as there are blades and the natural frequencies are very close together – in this case, the range is less than 200 Hz. At higher frequencies similar families of modes exist where each blade mode shape resembles a higher cantilever mode shape.

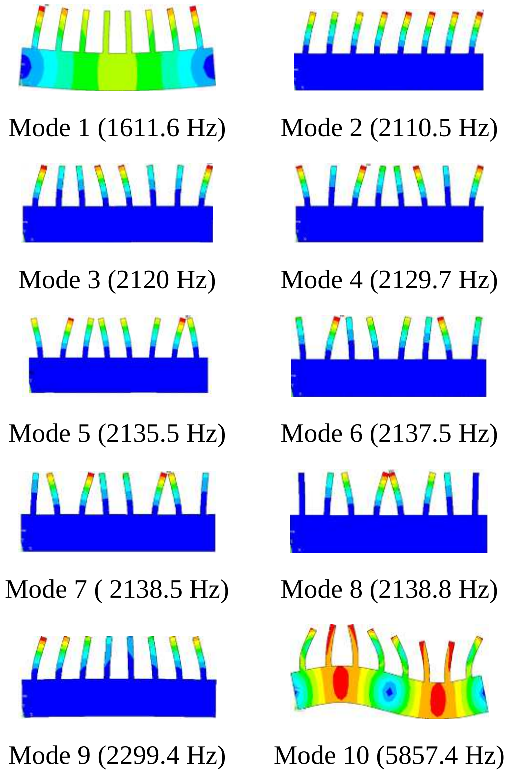

Figure 2: Modes of the comb structure

2.2 Modal Assurance Criterion and MAC/AutoMAC Plots

Changes in natural frequency can be quantified simply and used in damage identification algorithms. Changes in mode shape are less easy to quantify directly as they involve displacements at many points. One method for quantifying differences between mode shapes is the Modal Assurance Criterion (MAC). This quantity gives a scalar constant relating the degree of consistency (linearity) between one modal vector and another reference modal vector as defined by Equation 1:

$$\mathrm{MAC} = \frac{\left|(\Phi_1)^{\mathrm{H}}(\Phi_1)\right|^2}{(\Phi_1)^{\mathrm{H}}(\Phi_1)(\Phi_2)^{\mathrm{H}}(\Phi_2)} \tag{1}$$

where:

Φ_1 = First Modal Vector, Φ_2= Second Modal Vector

Use of the MAC and related approaches in model correlation is discussed extensively elsewhere [13-15]. For larger finite element models, calculation of the MAC can be cumbersome using modal vectors containing displacements for all active degrees of freedom (DOF). Additionally, small geometrical changes such as the addition of a crack to the model, can alter the number and order of nodes in a model resulting in inconsistent modal vectors. To alleviate this problem, modal vectors were created for a reduced set of nodes situated along the centrelines of each blade and the base or disc – see Figure 3.

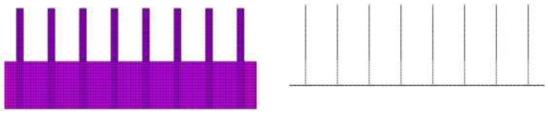

Figure 3: Comb structure complete mesh and skeleton.

To ensure that this reduction in the number of DOFs did not affect the ability to differentiate between modes, AutoMAC plots (a set of modes compared against themselves) for both the full and skeleton set of nodes were constructed – see Figure 4. The similarity of the two plots shows that this change in DOFs does not have a negative effect.

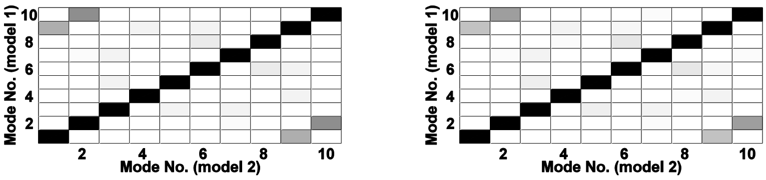

A B

Figure 4: Comparison of AutoMAC plots for the comb structure. (A) complete model and (B) model skeleton.

2.3 Crack model

Different techniques have been used in the past depending on whether the crack is open or breathing. For open cracks in beams, methods used have included: reduction in elastic modulus of selected elements, defining a pinned joint at a crack location using a rotational spring and material removal at the crack location. For breathing cracks, bilinear stiffness models have been used to represent opening and closing of a crack [16]. For development of damage identification strategies, it has also been suggested using plate-like structures, that a judicious addition of mass can provide an adequate estimate of the change in dynamics encountered [17].

Three crack modelling approaches were considered for simulating a crack in one of the blades of the comb structure – these are described below and shown in Figure 5.

a) Material removal at the crack location up to the required depth.

b) Reduction in modulus of elasticity involved changing the E value of elements in the vicinity of the crack depending on their average distance from the edge of the blade. The modulus was set at a very low value (near to zero) at the blade edge and incrementally increased up to the actual value for the blade at the crack tip. For example – if there were three elements representing a certain crack depth, then the modulus was set near to zero for the first element close to the blade edge while the second and third elements would have the modulus values equaling E/3 and 2E/3 respectively.

c) A lumped mass was attached near the blade tip. The mass was selected to give a similar frequency drop to the equivalent reduction in flexural stiffness.

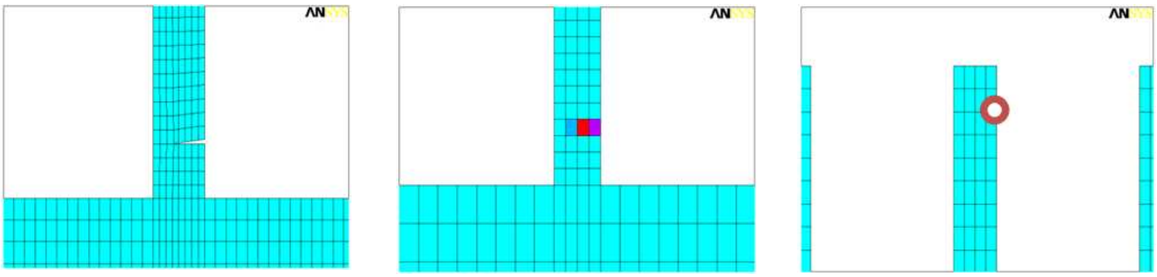

a. Material removal b. Reduction in E c. Lumped mass

Figure 5: Crack modelling approaches

A numerical comparison between the methods was carried out for the comb structure with a crack 6 mm above the root of the fifth blade on the left and extending through half the thickness of a blade. The resulting MAC plots are presented in Figure 6. They clearly show that each of the methods provides similar results.

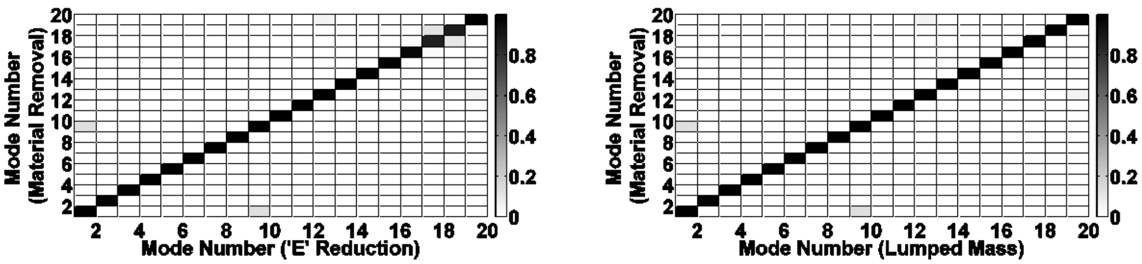

Figure 6: MAC plots for different crack modelling techniques.

Subsequent work was carried out using the material removal method. The crack depth and location parameters are shown in Figure 7.

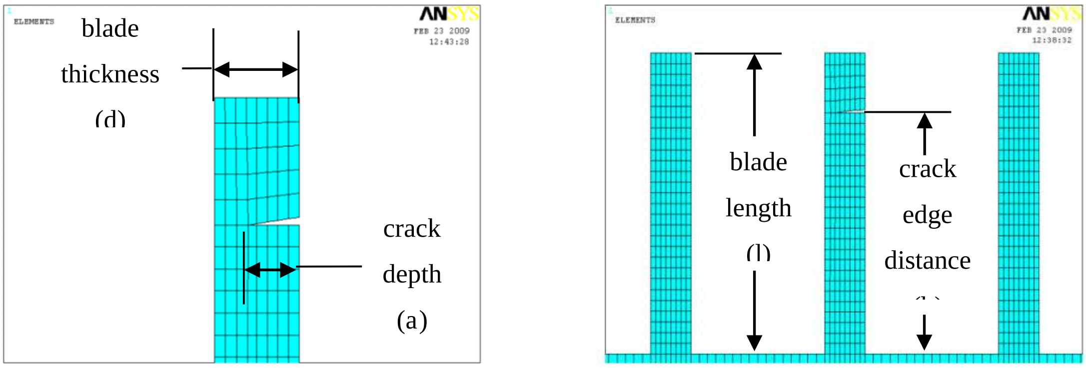

Figure 7: Crack depth and location parameters.

The FE analysis was rerun for the comb structure with a crack at b/l = 0.5. Figure 8 shows MAC plots between the original structure and the one with a cracked blade presented for two different crack depths a/d = 0.01 and 0.9. For the tiny crack (a/d = 0.01), the correlation between the sets of mode shapes is high although the presence of some off-diagonal terms indicates either some change or spatial aliasing. For the severe crack a/d = 0.9) the main diagonal is shifted downwards. In the first family of blade modes (2 to 9 in the undamaged set) seven of the eight modes are similar for both conditions. However the original Mode 9 is missing and a new mode has appeared at a lower frequency. This new mode is shown in Figure 9 where it is evident that it primarily involves motion of the damaged blade.

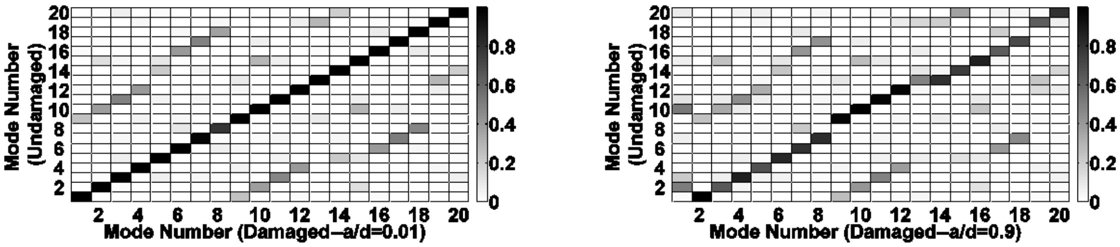

a- a/d = 0.01 **b-** a/d = 0.9

Figure 8: MAC plots between damaged and undamaged comb structure with b/l = 0.5

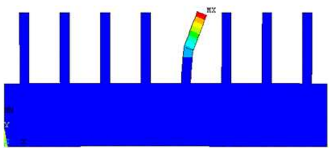

Figure 9: Damaged blade mode due to crack with a/d = 0.9 and b/l = 0.5

2.4 Damage index

While the MAC plots provide a good visual indication of change arising from damage, it is desirable to have a single scalar damage index. The damage index used here has shown encouraging results [18]. In this method, the MAC matrix is first subtracted from the auto-MAC matrix of the reference case. The resulting matrix represents the MAC change and gives a measure of disorder due to the presence of the crack. Initially, this change matrix was estimated by simply removing the main diagonal from the MAC matrix. However, it was found that because the AutoMAC includes off-diagonal terms as well as the main diagonal, the change matrix becomes a better measure of physical changes caused by damage. A single scalar value for this matrix is obtained by calculating its Frobenius norm which therefore provides a measure of the extent of that disorder. The Frobenius norm of a matrix is defined as the square root of the sum of the absolute squares of its elements. Its mathematical definition is given by Equation 2:

$$\|A\|_f = \sqrt{\sum_{i=1}^{m} \sum_{j=1}^{n} |a_{ij}|^2} \qquad (2)$$

For the comb structure, the damage index was calculated using the first 20 modes for cracks of various depth ratios (a/d = 0.01-0.9) and positions (b/l = 0.14, 0.5 and 0.8) on the fifth blade. Results are presented in Figure 10. It can be seen that the damage index is sensitive to crack depth even when the crack is small (b/l<0.1). This is particularly the case when the crack is nearer the root. In comparison, natural frequency changes were only evident in the cracked-blade mode discussed in the previous section whereas frequencies of the other modes changed by less than 0.1% even for very large cracks. For the cracked-blade mode, the frequency dropped as the crack depth increased. However, sensitivity was strongly influenced by location – to achieve a measurable 1% drop in frequency, crack depth ratios of 0.15, 0.28 and 0.9 would be required at locations b/1=0.14, b/l=0.5 and b/l=0.8 respectively.

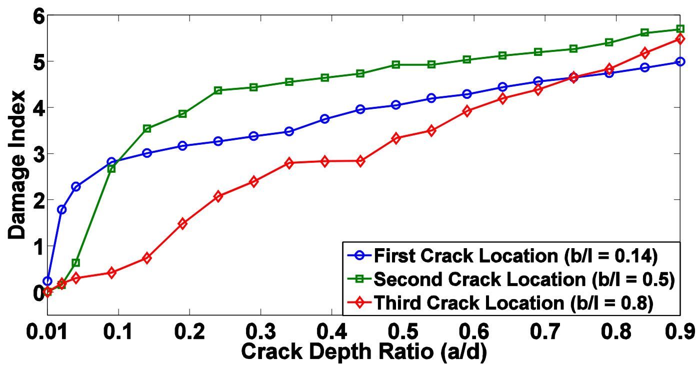

Figure 10: Damage index verses crack depth ratio (a/d) for comb structure

2.5 Uncertainty thresholds

The damage indices shown in Figure 10 assume perfect conditions; however, any changes in the MAC as a result of other environmental or operational variations in the structure may obscure the detection of damage. Temperature variations across an operating structure can usually cause problems for the damage detection algorithms as resulting stiffness variations alter natural frequencies. The sensitivity of the damage index to temperature change was investigated using the comb structure. It was found that uniform temperature changes across the structure did not affect mode shapes and hence the damage index. Instead, the structure was subjected to a sector-by-sector temperature gradient – effectively resulting in different Young's moduli for different sectors. Damage index values arising from different ranges in modulus values for an undamaged structure are shown in Table 1.

Young's modulus range (GPa)	0	2	6	10	20
Damage index	0	2.4	3.0	3.4	3.9

Table 1: Effect of varying Young's modulus on damage index

By using these in conjunction with the results for different cracks shown on Figure 10, it is possible to identify detectability thresholds for different crack locations and modulus (and hence temperature) uncertainty. For example, in this scenario with modulus uncertainty of 6 GPa, the smallest detectable crack would have a/d = 0.1 for Locations 1 and 2 but nearer 0.5 for Location 3.

2.6 Comment

To summarise; the crack initiation and propagation clearly altered the modal properties of the comb structure. Mode shapes were found to be more sensitive to the effect of the presence of a crack than the frequencies obtained after modal analysis of the structure. As far as crack depth and crack location are concerned, the natural frequencies decreased as cracks were propagated into the blade and this reduction was found to be more significant for crack locations near to the blade root as compared to crack locations near the blade tip. Similarly, any crack developed near the blade root resulted in a higher magnitude of damage index as compared to a crack developed near the blade tip. The damage index is correlated to the location and the depth of the crack.

3 Application to a bladed disc

The method developed in the previous section was next applied to a more representative structure – a solid disc with eight blades attached to it. The finite element model and skeleton set of DOFs were generated as for the comb structure. The geometry and mesh are shown in Figure 11. In the FE model, fixed boundary conditions were applied around the circumference of the central hole.

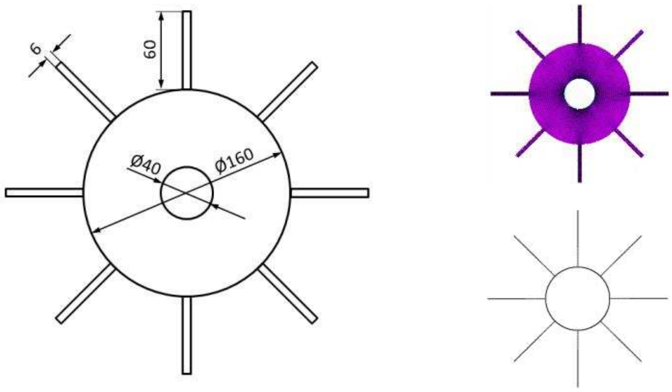

Figure 11: Dimensions, FE mesh and model skeleton of blade disc

3.1 Tuned bladed disc

Initially, the disc was studied with no mistuning present. The first nine natural frequencies are presented in Figure 12. It can be seen that Mode 9 is a disc-dominated mode. Modes 1 to 8 are the family of blade modes relating to the first flexure mode of a cantilever beam. The natural frequencies are even closer than for the comb structure with only 30 Hz separating all eight modes.

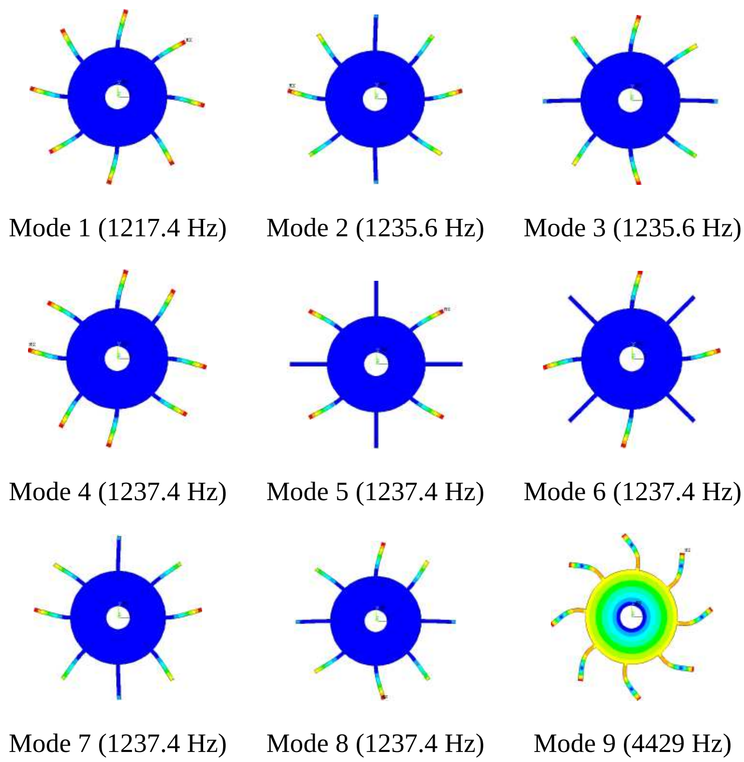

Figure 12: Mode shapes of the bladed disc

For the bladed disc model, cyclic symmetry of the structure gave rise to a complication when identifying nominally identical mode shapes using the MAC. Careful observation of Figure 12 shows that the only difference between Modes 2 and 3 is orientation – a quarter turn of one maps it onto the other. In a similar way, Modes 5 and 6 and Modes 7 and 8 are also identical pairs that can be overlaid by rotation around the centroid. This is a known feature of structures with perfect cyclic symmetry: when excited at natural frequency, the true operating deflection shape is the nominal mode shape rotated by an angle that depends on the forcing applied and is mathematically described as a combination of the two "identical" modes produced by the eigenvalue extraction routine. If the MAC is calculated directly, the correlation appears to be zero as different blades are in motion. To allow for rotational symmetry therefore, a modified procedure was followed. It can be noted that while the absolute circumferential position of the mode may vary, the relative movements of adjacent parts remains consistent. To allow for circumferential shifting to be applied more easily, modal displacements were first transformed to radial and tangential coordinates based on an origin at the centre of the disc. Modal vectors were constructed such that DOFs relating to a particular blade sector of the structure remained together and the relative positional order within the sectors was identical. For each mode, a total of eight modal vectors were created to represent the eight possible disc positions each with blade sectors appearing in a different order – as shown for Matrix B in Figure 13. Thus, rather than producing one MAC matrix between two sets of mode shapes, this procedure produced eight. The final step was to take the average MAC across the eight matrices. Where correlated modes occurred, the average MAC value was significantly higher than for uncorrelated modes because matching positions would give MAC values near 1. For the set of skeleton nodes for the eight bladed disc, correlated modes resulted in MAC values of around 0.9.

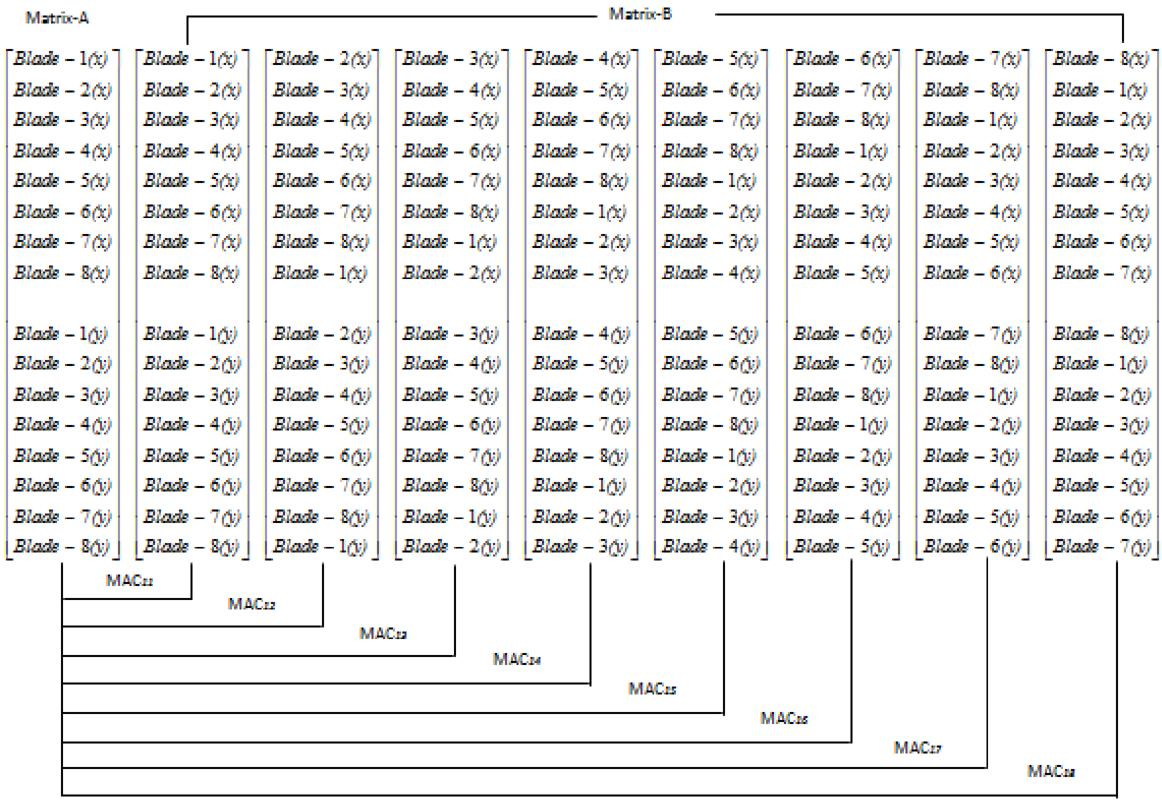

Figure 13: Assembling modal matrices for averaged MAC matrix.

Using the techniques developed earlier, the damage index was calculated for the bladed disc with cracks of different depth at different positions on one of the blades. Results are presented in Figure 14. It can again be seen that the damage index is sensitive to crack depth and that crack location is important. Note that even a very slight crack immediately altered the mode order – hence a damage index above 2 even for small cracks.

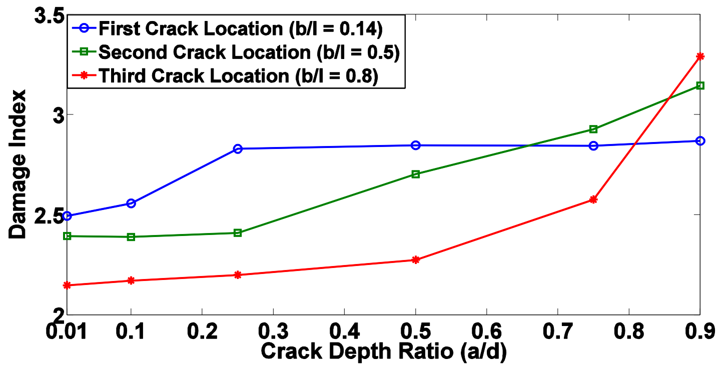

Figure 14: Damage index for the bladed disc.

3.2 Mistuned disc

Real bladed discs are never perfectly tuned. The effect of mistuning on the ability of the method to detect damage was investigated by considering scenarios with different mistuning patterns achieved by attaching lumped masses arbitrarily to certain blade tips. Three different mistuning patterns are shown in Figure 15. It is useful to note here that a 0.1g lumped mass attached to one of the blade tips results in a frequency drop of approximately 1.2%.

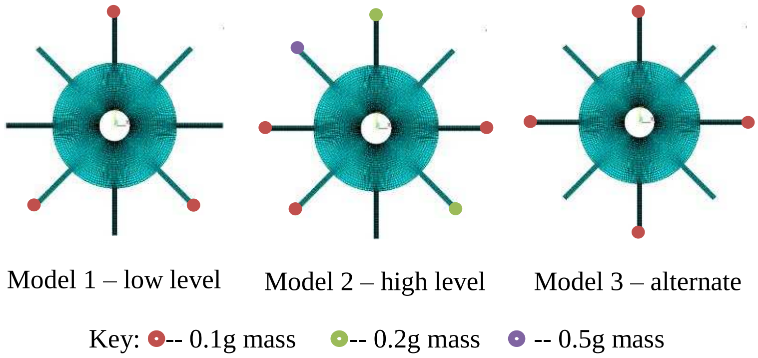

Figure 15: Bladed disc mistuning patterns.

Modal characteristics of the three mistuned conditions were obtained numerically. With the added mistuning, the frequency range over the first family of blade modes increased from 30 Hz in the tuned model to 70 Hz for Models 1 and 3 and 140 Hz for Model 2. Also, by upsetting the symmetry of the disc, the blade mode shapes were changed with individual blades moving by different amounts.

The damage index was calculated using the MAC matrix between the perfectly tuned bladed disc without any crack and the mistuned system with cracks. Results are shown in Figure 16. It can be seen that the presence of low and high levels of mistuning in the bladed disc resulted in almost the same values of damage index for the entire range of crack depth ratios considered.

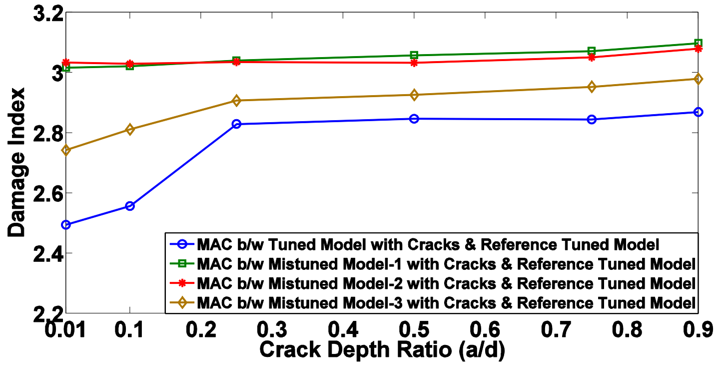

Figure 16: Damage index plot for mistuned bladed disc

The alternately mistuned system indicated a lower magnitude of the damage index. Furthermore, the trend of the curve for the alternately mistuned system bears a similarity to the curve obtained for the perfectly tuned system, making the effect of mistuning less severe. As the damage index plots are strictly dependent on the mode shapes obtained, higher magnitudes of the damage index can be attributed to the presence of localised modes due to mistuning. For mistuned models, localisation of vibration energy occurred according to the mistuning pattern present.

3.3 Blade tip data for mistuned disc

In practice, it is rare to have detailed mode shape information at many points on a structure. In order to investigate the applicability of the MAC-based crack detection method considering limited data that could be obtained from current measurement technology such as blade tip timing, a reduced data set was acquired that contained information from the tips of the blades only. The damage index against crack depth ratio plot is shown in Figure 17.

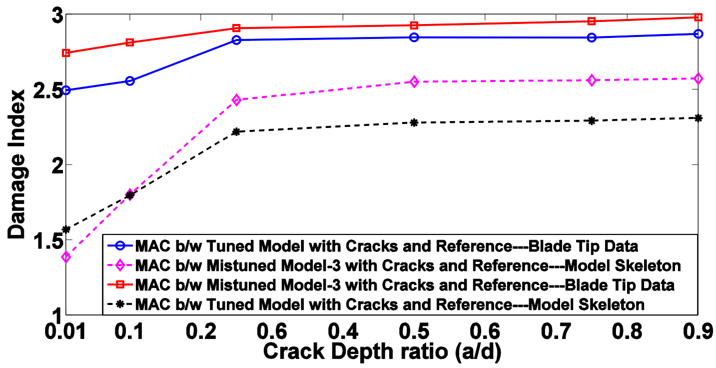

Figure 17: Damage index plot using blade tip data.

It can be seen that data from the blade tips indicated more sensitivity to the presence of damage resulting in higher magnitudes of the damage index in comparison to the model skeleton approach. In addition to that, tip data was more effective for damage detection in the mistuned bladed disc as compared to the tuned bladed disc as it resulted in higher magnitudes of the damage index for the mistuned system. A likely reason for this result is that for the modes considered, blade tips provide the greatest difference in shape. Therefore, for a blade mode family with more significant mid-blade motion, this finding may not hold as true.

3.4 Comment

To summarise; the presence of mistuning altered the modal characteristics of the bladed disc by localising the vibration modes and, therefore, resulted in non-uniform distribution of vibration energy across the whole structure. These localised modes resulted in higher magnitudes of damage index. In addition, the effect of the presence of a crack on the modal characteristics of bladed disc was overwhelmed by the presence of mistuning in the structure. This phenomenon varied according to the pattern and level of mistuning inside the bladed disc. Data from blade tips proved to useful for generating damage index plots, especially in the presence of mistuning.

4 Experimental validation

The purpose of this step was to show that the models used in previous stages were reasonable and that the method works for experimentally obtained data.

The experimental bladed disc was manufactured using electro-discharge machining (EDM) from a medium carbon steel disc 40 mm in thickness. The dimensions of the specimen were nominally the same as the FE model of the bladed disc, except for the diameter of the hole in the centre of disc which was reduced from 40 mm to 8 mm. The disc was fixed to a heavy steel table to simulate a rigid support. Note that washers were used to keep the disc face away from the table.

A roving hammer test was then used to obtain the frequency response of the disc at 48 different positions (six per blade). A picture of the test assembly is provided in Figure 18.

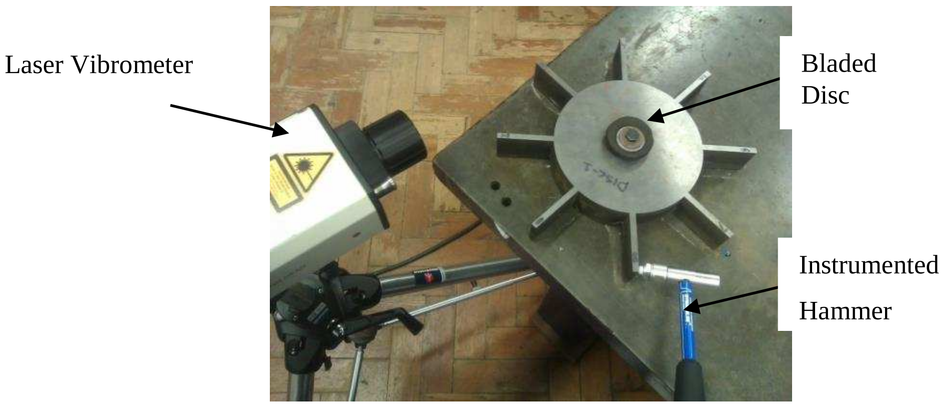

Figure 18: Bladed disc specimen and experimental setup.

Excitation was provided using a nylon-tipped hammer that was instrumented with a force transducer. The response was measured using a single-point laser vibrometer. For each impact, measurements were acquired over a time period of 2 seconds using a sampling rate of 8192 Hz. When calculating the FRFs, rectangular windows were used with both force and velocity traces as the signal to noise ratio was high and the vibration died away within the acquisition time frame. A typical FRF of the bladed disc is shown in Figure 19 – where the group of peaks in the range 1230-1300 Hz relate to the first family of blade modes. It is interesting to note that these measured resonances occur in the same frequency range as the predicted blade modes. Additionally, the spread of 70 Hz between lowest and highest modes in that family matches that seen for the model when mistuning was light (configurations 1 and 3).

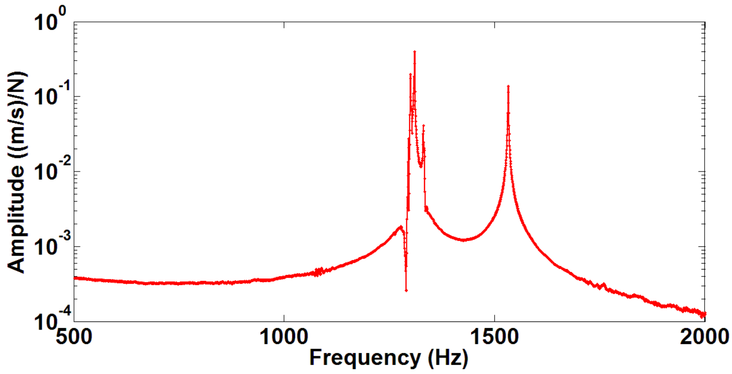

Figure 19: Typical experimental FRF of the bladed disc specimen.

Careful measurement of the blades showed that there was some variation in thickness – arising from the release of residual stresses during the EDM process – which resulted in mistuning of the disc. Because of this, a direct comparison between measured and predicted natural frequencies and modes shapes would not necessarily give a close correlation. Instead, the natural frequencies of individual blades were compared. Experimentally, this was achieved on a blade-by-blade basis by attaching heavy magnets to the other seven blades to move their resonances to different frequency ranges. Note that because the damping ratio for each mode was in the range 0.0001-0.0005, it could be assumed that the resonance frequency and natural frequency were identical. Theoretical predictions were made using the average measured thickness for each blade rather than the nominal value. A comparison of measured and predicted results for the individual blade modes are given in Table 2. Close correlation gives confidence in both experimental and theoretical results.

	Blade number									
	1	**2**	**3**	**4**	**5**	**6**	**7**	**8**	Mean	Standard deviation
Predicted	1317.4	1305.3	1300.9	1303.8	1313.5	1305.2	1300.0	1306.0	1306	6.0
Measured	1308.7	1291.3	1308.4	1297.6	1311.9	1310.6	1308.4	1314.7	1306	7.9

Table 2: Natural frequencies of individual blades in Hz (prediction based on nominal geometry is 1310 Hz)

The final step in this demonstration was to investigate the performance of the damage index using experimental data. Rather than attempt to induce a crack in the specimen, a light mass was added to a blade to generate a "pseudo-fault". This was shown in Section 2 to have a similar effect on the damage index as a real crack. Using the FE model of the bladed disc, it was found that the addition of a 10 gram mass at the tip of a blade had the same effect as a large crack with a/d = 0.5 located at b/l = 0.14. For reference, a comparison of the natural frequencies is given in Table 3.

	Mode Number									
	1	**2**	**3**	**4**	**5**	**6**	**7**	**8**	**9**	**10**
a/d = 0.5	683.5	1120.1	1277.5	1278.7	1280.2	1280.3	1280.3	1281.4	1567.1	1998.6
10g mass	676.47	1120.3	1277.5	1278.7	1280.2	1280.3	1280.3	1281.4	1570.9	1966.2

Table 3: Natural frequencies comparison for a/d = 0.5 and 10g mass.

Once the mass was attached to the blade, the roving hammer test was repeated for all 48 points. For both the undamaged and "damaged" cases, the first eight modes were extracted using the PolyMax algorithm provided by the LMS software. The damage index calculated from these mode shapes was 4.18. In order to provide a threshold for comparison, the damage index was also calculated using the numerical and experimental mode shapes for the undamaged case. This gives a value of 1.63 – effectively a measure of the disorder created by the mistuning present. The result is also illustrated in Figure 20 and shows that the detection method devised can identify damage from experimental data despite the presence of uncertainty from mistuning.

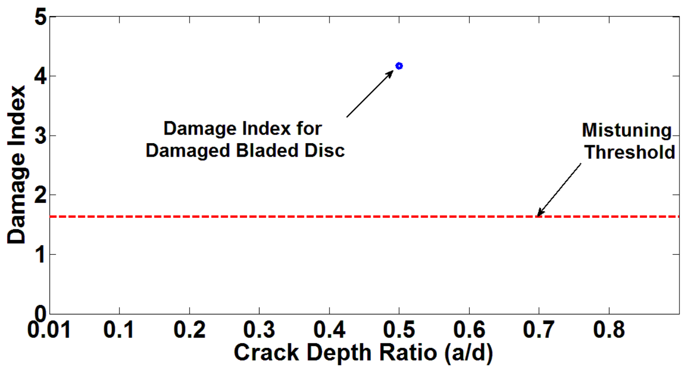

Figure 20: Damage index verses crack depth ratio plot with mistuning threshold.

5 Conclusions

An investigation, using the Modal Assurance Criterion, of cracks and mistuning in repeating structures has been carried out in this paper. A damage index was correlated to the location/depth of crack and level/pattern of mistuning present inside the system. The presence of a crack and mistuning altered the modal characteristics of the repeating structure. Mode shapes were found to be more sensitive to the location and depth of crack as compared to the natural frequencies. Amongst various crack modelling techniques considered, a material removal method was selected to model cracks in repeating structures. Any crack developed near the blade root resulted in higher magnitudes of damage index as compared to cracks near the blade tips. The presence of mistuning caused mode localisation phenomenon, which resulted in higher magnitudes of the damage index. In addition to that, the effect of the presence of a crack on the modal characteristics of the bladed disc was overwhelmed by the presence of mistuning in the structure. This phenomenon varied according to the pattern and level of mistuning. The MAC-based investigation technique worked well for the experimental data. The level of mistuning is identified by obtaining an approximation for the manufacturing tolerance and material degradation-induced mistuning, which can provide a baseline for highlighting a crack of certain depth in a mistuned bladed disc. A threshold to identify a crack in the mistuned environment of the bladed disc can be obtained by mistuning identification and plotting it on damage index curves. Data from blade tips proved to useful for generating damage index plots for the bladed disc, especially in the presence of mistuning.

REFERENCES

[1] J. Pitkanen, T. Hakkarainen, NDT methods for revealing anomalies and defects in gas turbine blades, , Insight: Non-Destructive Testing and Condition Monitoring, Vol. 43 (9), (2001), pp 601-604.

[2] J. Hou, Cracking-Induced Mistuning in Bladed Disks, AIAA Journal , Vol. 44 (11), (2006), pp. 2542-2546.

[3] S. Kumar, N. Roy, Monitoring Low Cycle Fatigue Damage in Turbine Blade using Vibration Characteristics, Mechanical Systems and Signal Processing, Vol. 21 (1), (2007), pp. 480-501.

[4] O. S. Salawu, Detection of structural damage through changes in frequency: a review, Engineering Structures, Vol. 19, No. 9, (1997), pp. 718-723.

[5] M. Chatti, R. Rand, S. Mukherjee, Modal Analysis of a Cracked Beam, Journal of Sound and Vibration, Vol. 207(2), (2007), 249-270

[6] J. Slastan, S. Pietrzko, Changes of RC-beam modal parameters due to cracks. Proceedings, 11th International Modal Analysis Conference, Kissimmee, Florida (1993), pp. 70–76.

[7] R.D. Begg, A.C. Mackenzie, C.J. Dodds and O. Loland, Structural integrity monitoring using digital processing of vibration signals, Proceedings, 8th Offshore Technology Conference, Houston, Texas, (2002), pp 305-311..

[8] A. U. Rehman, J. A. Rongong, K. Worden, Amplitude dependent crack characterization of growing fatigue cracks. Rotating Machinery, Structural Health Monitoring, Shock and Vibration, Vol. 5, (2011), pp 83-92.

[9] Z. K. Peng, Z. Q. Lang, Crack detection using nonlinear output frequency response function, Journal of Sound and Vibration, Vol. 310, (2007), pp 777-788.

[10] S. Campobasso, M. Giles, Analysis of the effect of mistuning on turbomachinery aeroelasticity, Proceedings of the 9th International Symposium on Unsteady Aerodynamics, Aeroacoustics and aeroelasticity in Turbomachines, Presses University of Grenoble, Grenoble, France, (2001), pp. 885-886.

[11] M. I. Hussein, C. Pierre, Examination of the relationship between tuned free vibration characteristics and mistuning sensitivity for an industrial turbomachinery rotor, Report Number UM-ME-01-06, Department of Mechanical Engineering, The University of Michigan, USA, (2001).

[12] M. P. Castanier, C. Pierre, Modelling and analysis of mistuned bladed disk vibration: status and emerging directions, Journal of Propulsion and Power, Vol. 22 (2), (2006), pp. 384-396.

[13] R. J. Allemang, The modal assurance criterion: twenty years of use and abuse, Proceedings of, IMAC-XX: A Conference and Exposition on Structural Dynamics, Los Angeles, USA, (2002), pp. 397–405.

[14] D. Fotsch, D. J. Ewins, Further applications of the FMAC, Proceedings of IMAC XIX, (2001), pp. 635-639.

[15] D. Fotsch, D. J. Ewins, Application of MAC in Frequency Domain, Proceedings IMAC XVIII, Vol 4062, (2000), pp. 1225.

[16] M. I. Friswell, J. E. T. Penny, Crack Modelling for Structural Health Monitoring, Journal of Structural Health Monitoring (SHM) Vol 1(2), (2002), pp. 139-148.

[17] E. Papatheou, G. Manson, R. J. Barthorpe, K. Worden, The use of pseudo-faults for novelty detection in SHM, Journal of Sound and Vibration, Vol. 329 (12), (2010), pp. 2349-2366.

[18] A. U. Rehman, J. A. Rongong, and K. Worden, Detection of Damage in Repeating Structures, Proceedings of the ASME Turbo Expo 2010: Power for Land, Sea and Air, GT 2010, Glasgow, UK, Vol. 6, (2010), pp. 1053-1061.

Appendix – A

Natural frequencies (Hz) for different mistuning patterns in the bladed disc.

Mode number	Tuned system (without crack)	Tuned system (with crack)	Arbitrarily (low level) mistuned system	Arbitrarily (high level) mistuned system	Alternately mistuned system
1	1217.4	1162.8	1093.5	955.24	1093
2	1235.6	1220.4	1157.1	1034.9	1155
3	1235.6	1235.6	1162.1	1096.8	1162
4	1237.4	1236.1	1225.8	1155.7	1162
5	1237.4	1237.4	1236	1161.5	1228
6	1237.4	1237.4	1236.5	1162.4	1237
7	1237.4	1237.4	1237.4	1232.8	1237
8	1237.4	1237.4	1237.4	1236.6	1237
9	4429	4428.3	4416.5	4386.4	4412
10	7265.3	7261.5	6960.6	6317.1	6962
11	7265.3	7265.3	7008	6715.6	6973
12	7444.2	7435.9	7142.4	6819	7052

a- a/d = 0.25, b/l = 0.14

Mode number	Tuned system (without crack)	Tuned system (with crack)	Arbitrarily (low level) mistuned system	Arbitrarily (high level) mistuned system	Alternately mistuned system
1	1217.4	1214.3	1145.5	955.25	1144.9
2	1235.6	1227	1157.8	1083.3	1156.4
3	1235.6	1235.6	1162.1	1097	1161.7
4	1237.4	1236.2	1226	1155.8	1162.2
5	1237.4	1237.4	1236	1161.5	1228.5
6	1237.4	1237.4	1236.5	1162.4	1236.5
7	1237.4	1237.4	1237.4	1232.8	1236.5
8	1237.4	1237.4	1237.4	1236.6	1237.4
9	4429	4426.3	4413.7	4383.1	4409.7
10	7265.3	7056	6720.4	6316.2	6720.7
11	7265.3	7265.3	7008	6480.4	6972.6
12	7444.2	7339.1	7097.4	6799.3	7030.8

b- a/d = 0.25, b/l = 0.5

Mode number	Tuned system (without crack)	Tuned system (with crack)	Arbitrarily (low level) mistuned system	Arbitrarily (high level) mistuned system	Alternately mistuned system
1	1217.4	1217.5	1154.9	955.25	1152.7
2	1235.6	1235.6	1162.1	1094.9	1161.7
3	1235.6	1235.8	1162.1	1098.8	1161.9
4	1237.4	1237.4	1226	1155.9	1162.7
5	1237.4	1237.4	1236	1161.5	1228.6
6	1237.4	1237.4	1236.5	1162.4	1236.5
7	1237.4	1237.4	1237.4	1232.8	1236.5
8	1237.4	1238.1	1237.4	1236.6	1237.4
9	4429	4428.8	4416.5	4386.1	4412.6
10	7265.3	7248.5	6925.5	6317	6927.6
11	7265.3	7265.3	7008	6670.1	6972.6
12	7444.2	7414.5	7127.5	6809.6	7043

c- a/d = 0.25, b/l = 0.8